Balance of Upper Limb Muscle Activation and Aerodynamics for Cycling Posture Optimization

Xiangru Li[a], Peng Zhou[b] and Xin Zhang[c]

Department of Mechanical and Aerospace Engineering, The Hong Kong University of Science and Technology, Clear Water Bay, Kowloon, Hong Kong SAR, China

Keywords: Aerodynamics, Cycling Postures, Electromyography, Performance Optimization.

Abstract: Cycling postures significantly influence aerodynamic performance in competitive cycling, yet aggressive postures may increase muscle activation and lead to adverse physiological effects. This study evaluated the aerodynamic drag area (C_dA) of various cycling postures in a wind tunnel, revealing a strong correlation with decreasing forearm angles. Surface electromyography (sEMG) tests were conducted to assess upper limb muscle activation across postures, identifying the triceps brachii (TB) as dominant in maintaining both hoods and drops positions (46.9% and 40.2% of total activation, respectively). Additionally, this study explores the trade-off between aerodynamic gains and muscle activation by examining the relationship between C_dA and composite EMG. A Pareto front analysis identified locally optimal postures that balance these factors, potentially enhancing overall cyclist performance.

1 INTRODUCTION

Cycling performance is influenced by a multitude of factors, including psychological, physiological, biomechanical, and environmental conditions (Berry et al., 1994; Ghasemi et al., 2022; Arpinar-Avsar et al., 2013). A key determinant of cycling performance, cycling speed, depends on the cyclist's power output, aerodynamic drag, and environmental factors such as wind and terrain (Martin et al., 2006). Approximately 90% of the total resistance experienced during cycling at a speed over 30 km/h on flat road arises from the combined aerodynamic drag of the cyclist and their equipment (Faria et al., 2005). While innovative equipment—such as aerodynamic helmets, aero handlebars, and skinsuits—can reduce drag to some extent, cycling postures remain a critical factor in refining the human-equipment interaction. Short-distance sprint events often prioritize power output, whereas endurance time trials (TTs) require a balance between physiological efficiency and aerodynamics (Faulkner et al., 2024; Fintelman et al., 2014).

Altering cycling postures primarily involves adjustments of torso and hip angles (Fintelman et al., 2014, 2015). Aerodynamically favorable positions typically require cyclists to adopt a crouched posture, with the forearm and trunk positioned nearly parallel to the ground. However, such positions can compromise critical power output. For instance, transitioning from the hoods of the handlebar to a TT position has been shown to reduce critical power (Kordi et al., 2019). Furthermore, aggressive postures may adversely affect physiological metrics, including oxygen consumption, muscle activation, muscle pain and injury risk, and overall cycling economy (Turpin et al., 2017; Faulkner and Jobling, 2020; Brand et al., 2020). Muscle activity, commonly measured using surface electromyography (EMG), is associated with both fatigue, pain, and injury (Streisfeld et al., 2017) and power production. For instance, a lower hip angle can reduce muscle activation, thereby decreasing lower limb power output (Kordi et al., 2019; Moura et al., 2017). However, the effects of posture alterations on muscle activity remain equivocal. Bini et al. (2019) assessed the influence of different hip flexion angles on muscle forces, reporting that changes in upper body position by varying hip angles altered contributions of the knee and hip joints without impact on peak muscle forces. In contrast, Dorel et al. (2009) found that aero position significantly increased EMG activity level of *gluteus maxiums* and *vastus medialis*, compared with upright posture, while gas-exchange variables presented minor differences.

Maintaining an aerodynamic position without specialized equipment, such as aero handlebar, is widely recognized as challenging and often leads to exces-

[a] https://orcid.org/0009-0003-1601-2751
[b] https://orcid.org/0000-0003-4936-9661
[c] https://orcid.org/0000-0001-9322-4115

Li, X., Zhou, P. and Zhang, X.
Balance of Upper Limb Muscle Activation and Aerodynamics for Cycling Posture Optimization.
DOI: 10.5220/0013677000003988

In *Proceedings of the 13th International Conference on Sport Sciences Research and Technology Support (icSPORTS 2025)*, pages 50-56
ISBN: 978-989-758-771-9; ISSN: 2184-3201

sive upper body muscle activation, potentially causing pain and fatigue (Turpin et al., 2017; Brand et al., 2020). This discomfort typically stems from prolonged cervical spine extension and lumbar spine hyperflexion, which impose high loads and compression on surrounding muscles during forward leaning (Dettori and Norvell, 2006; Schwellnus and Derman, 2005). Identifying an optimal cycling posture remains a complex challenge, as it requires balancing power output, aerodynamics, and comfort (Savelberg et al., 2003; Umberger et al., 1998; Brand et al., 2020). Most previous studies on the impact of posture on performance have focused on professional cyclists or the lower limbs (Berry et al., 1994, 2000; So et al., 2005). Moreover, adaptations to specialized equipment and aggressively crouched positions through regular training may not generalize to recreational cyclists, highlighting the need for further research on upper body and recreational population (Ashe et al., 2003; Brand et al., 2020; Chapman et al., 2008; Savelberg et al., 2003).

Despite these insights, there remains a scarcity of research addressing the balance between aerodynamic optimization and physiological cost. Faulkner et al. (2020) introduced the concept of aerodynamic-physiological economy (APE), which integrates metabolic costs, aerodynamic positioning, and their interaction with TT performance, providing valuable predictions of cycling efficiency across varying upper body postures . However, their drag area (C_dA) estimates relied on anthropometric data and measured frontal area, which may lack precision. Giljarhus et al. (2020) explored the drag effects of adjusted arm positions using computational simulations, but such methods may overlook complex real-world flow conditions requiring further experimental validation. Faulkner et al. (2024) later advanced aerodynamic measurement by integrating a commercial device on the base bar of a bicycle during TT experiments . However, this approach may not fully capture the aerodynamics of the entire bike-rider system, underscoring the need for more accurate drag measurements.

This study aims to investigate the effects of cycling posture alterations on aerodynamic drag and upper limb muscle activity in recreational cyclists. It first examines the relationship between muscle activation contributions, forearm angles across posture variations, and aerodynamic drag, and further analyzed data using Pareto optimization in search of optimal postures. We hypothesize that the biceps brachii and triceps brachii muscles will contribute the majority of activation among the measured upper limb muscles, and that aerodynamic drag-muscle activity will manifest a linear relationship.

2 MATERIALS AND METHODS

2.1 Participants

Nine young male cyclists (age = 27.1 $\pm$ 2.0 years, height = 180.0 $\pm$ 6.3 cm, weight = 77.0 $\pm$ 5.7 kg, mean $\pm$ SD) from the Hong Kong University of Science and Technology (HKUST) voluntarily agreed to participate in this study. A priori sample size calculation (G*Power, version 3.1.9.7, Kiel, Germany) determined that 9 participants would provide 80% (α = 0.05) to achieve an effect size = 0.8 in muscle activation. Inclusion criteria required participants to be competent in riding a bicycle without prior or current professional training. Exclusion criteria included any chronic or acute muscle injuries or mental disorders that could adversely affect cycling performance. This study was approved by the Human and Artefacts Research Ethics Committee of HKUST (HREP-2023-0145) and conducted in accordance with the ethical principles of the Declaration of Helsinki. Written informed consent was obtained from all participants prior to the study.

2.2 Protocol

All subjects were invited to attend three experimental sessions. Session I measured aerodynamic drag in a wind tunnel (see Sec.2.3), while session II and III assessed muscle activity (see Sec.2.4) on a bike trainer (Wahoo Kickr Bike, Atlanta, USA) in the hoods and drops hand position, respectively. The bike trainer, located in an air-conditioned room of 23 °C, has a power accuracy of $\pm 1\%$.

In session I, all participants were asked to wear cycling skinsuits, cycling shoes and road bike helmets that fitted to their individual body sizes to minimize the aerodynamic influence of personal garments. They exercised on a fixed road bike positioned in the wind tunnel, pedaling to drive the rear wheel at a speed matching the wind tunnel's airflow. Participants maintained 10 distinct postures with varying forearm angles in the hoods hand position, each held for 30 s, with 30 s rest intervals between randomly sequenced postures. The same procedure was then repeated for 10 postures in the drops hand position. Figure 1 shows the postures adopted in the tests in hoods and drops position, respectively. Posture 1 presents a maximum forearm angle, equivalent to an upright posture without arm bending. Posture 10 presents a minimum forearm angle. The forearm angle is defined as the acute angle between a subject's forearm and a horizontal line, as shown in Fig.1a.

In Session II, participants replicated the 10 hoods postures from the wind tunnel test in a randomized order to reduce order effect. They performed these postures on the bike trainer at a constant power output of 100 W, pedaling at 60 rpm, a low exercise intensity intended to reduce the impact of lower limb fatigue on RPE evaluation. To mitigate fatigue effects on subsequent trials, a stop criterion was applied: participants could end a trial either after maintaining a posture for 2 min or upon self-reporting a rated perceived exertion (RPE) score of around 14 (equivalent to "somewhat hard" to "hard" on the Borg scale (Borg, 1982)). Each trial was separated by a 3 min rest period. Session III followed the same protocol as session II, but with the drops hand position. For both session II and III, participants were instructed to refrain from high-intensity exercise for at least 24 hours prior to laboratory trials. Session II and III were conducted separatedly by at least 48 hours and were randomly assigned to each participant.

2.3 Aerodynamic Force Measurement

Aerodynamic drag was measured in a low-speed wind tunnel at the Aerodynamics and Acoustics Facility (AAF), HKUST. The wind tunnel featured a closed test section measuring 14 m $\times$ 2.5 m $\times$ 2 m. All measurements were conducted at a constant wind speed of 8 m/s, representative of typical leisure cycling speeds. A road bike was mounted on a cycling aerodynamic test rig installed underneath the wind tunnel floor for force measurements. Loads were recorded using a six-component force balance with a measurement accuracy within ± 0.2 N (Mao et al., 2024). Each force measurement was sampled 2 000 Hz for a duration of 30 s.

2.4 EMG Recording

Muscle activity is measured using a surface EMG device (Cometa Systems PicoX and miniX, Bareggio, Italy) with a sampling frequency of 2 000 Hz per channel. EMG was recorded for six muscles on the participants' dominant side of the body: *flexor carpi radialis* (FCR), *biceps brachii* (BB), *medial triceps brachii* (TB), *anterior deltoids* (AD), *upper trapezius* (UP) and *lumbar erector spinae* (ES). Prior to electrode application, the skin was shaved and cleaned with alcoholic pads. A bilateral Ag/AgCl monitoring electrode (3M Red Dot, MN, USA) was placed in the middle of the muscle belly according to the sEMG

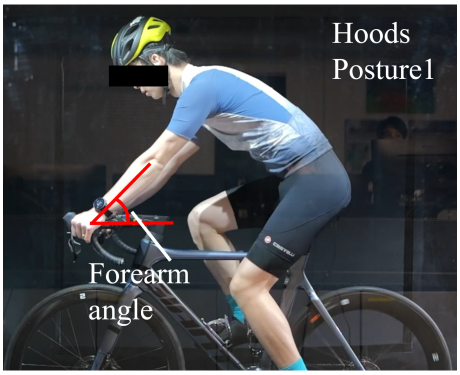

(a)

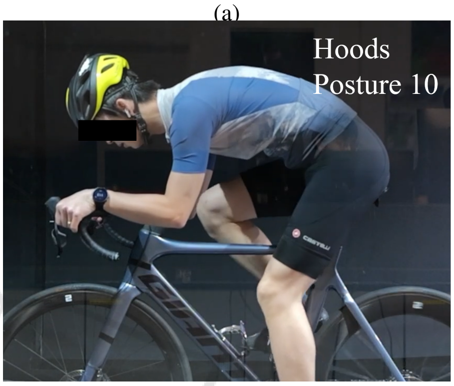

(b)

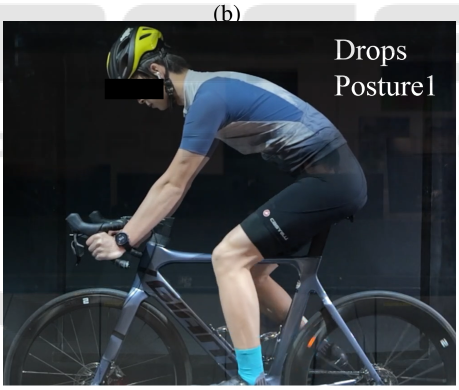

(c)

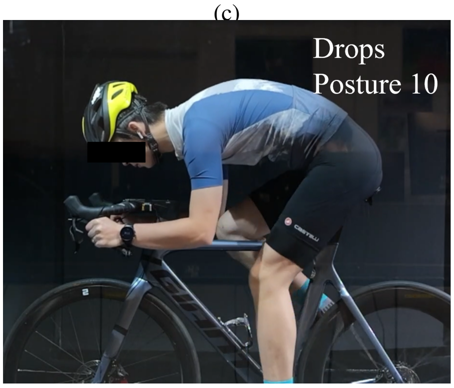

(d)

Figure 1: Postures in hoods and drops position.

application standards (Stegeman and Hermens, 2007).

2.5 EMG Data Processing

Raw EMG signals were band-pass filtered using a 4th-order Butterworth filter between 20 and 500 Hz, followed by full-wave rectification and root mean square (rms) calculation with a window size of 0.5s, as shown in Fig. 2. For each participant and for each muscle, rms EMG was further normalized by its dynamic peak to obtain EMG linear envelope (Burden and Bartlett, 1999). The dynamic peak was determined in a separate trial, where participants crouched their upper body to the lowest position, maximally contracted the target muscle, and pedaled at full power for 10 s, this process was repeated three times, and the average of the three trials was used as the dynamic peak value.

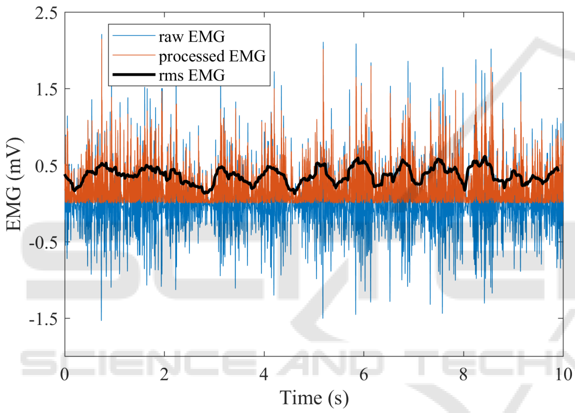

Figure 2: Sample EMG of TB muscle from a participant in drops posture 7. Processed EMG refers to the rectified EMG before performing rms calculation.

To assess the variation in muscle contributions supporting upper body postures, muscle activation weights were calculated as follows:

$$\text{Weight}_i = \frac{\text{rms EMG}_i}{\sum_{j=1}^{6} \text{rms EMG}_j}, \tag{1}$$

where Weight$_i$ represents the contribution of the i^{th} muscle, and the denominator is the sum of root mean square EMG values across all measured muscles.

The composite sum of the EMG signals was computed to estimate overall muscle activity across the measured muscle (Ingraham et al., 2019), defined as:

$$\text{Composite rms EMG} = \sqrt{\sum_{i=1}^{6} \text{rms EMG}_i^2}, \tag{2}$$

where i denotes i^{th} muscle ranging from 1 to 6 (corresponding to the six muscles recorded).

2.6 Pareto Optimality Analysis

Pareto optimality, a foundational concept in economics and management science, was introduced by Pareto (1919). In multi-criteria decision-making, a solution is considered Pareto optimal if no other solution is at least as good across all criteria and better in at least one criterion (Ehrgott, 2005). This is mathematically expressed as:

$$min\{f_1(y), f_2(y), \ldots, f_m(y), f_M(y)\}, \tag{3}$$

where $y = (y_1, y_2, \ldots, y_n)$ represents the decision variables, f_m denotes the objective functions, $1 \leq m \leq M$ and $M \geq 2$. In this context, $M = 2$, as two objective functions were considered: drag area (C_dA) and the composite sum of EMG.

3 RESULTS AND DISCUSSION

3.1 Aerodynamic Drag and Postures

Aerodynamic drag measurement were performed at wind speed of 8m/s. The drag area C_dA is defined as

$$C_dA = \frac{2F_d}{\rho U_0^2}, \tag{4}$$

where F_d is the measured mean drag force, ρ is the air density and U_0 denotes the flow speed at the wind tunnel outlet.

Figure 3 illustrates the variation in C_dA across descending forearm angles. The shaded regions represent 95% confidence intervals, while data of all participants are shown as dots. Both hoods and drops positions exhibited a strong correlation between C_dA and decreasing forearm angles. This indicates that lowering the forearm angle and adopting a more crouched upper body posture significantly reduces drag area, thereby enhancing cycling performance. The consistent correlation across positions suggests that posture optimization is a critical factor in aerodynamic efficiency.

3.2 Muscle Activation

Figure 4 illustrates the changes in muscle activation weights for each measured muscle across postures, with posture indices 1 to 10 corresponding to a shift from an upright posture (maximum forearm angle) to an aerodynamic posture (minimum forearm angle). Error bars represent 95% confidence intervals. The results reveal that the TB muscle was the primary contributor to overall muscle activity, accounting for

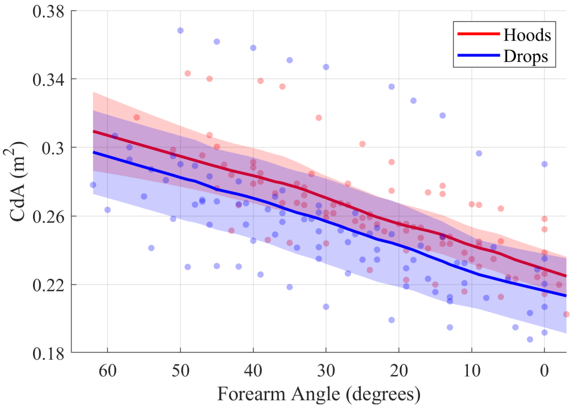

Figure 3: Drag area (C_dA) versus forearm angles in increased crouching down. Data of all participants are shown as dots.

46.9% and 40.2% of activation in the hoods and drops positions, respectively. In the hoods position, TB activation typically increased as postures became more aerodynamic, despite minor fluctuations. Conversely, in the drops position, TB activation decreased after posture 7, possibly due to accelerated fatigue from increased torso forward tilt, which heightens upper arm loading to support body weight. Moreover, it is observed that arm and chest muscles (FCR, BB, and AD) were more recruited in drops, whereas shoulder and back muscles (UT, and ES) showed greater activation in hoods.

3.3 Drag-Muscle Activity Relationship

Figure 5 displays the relationship between aerodynamic drag and muscle activity, with data averaged across participants for each posture. The composite sum of EMG, representing total upper body muscle activity, is plotted against C_dA. Figure 5a shows the Pareto front for individual participant (in colored dash line) and the group trend (in red solid line). The findings suggest that drops postures generally provide a better balance between aerodynamic drag and muscle activity in a crouched position, compared to hoods within the measured forearm angle range. On the other hand, as the upper body shifts to a more upright posture, hoods postures' Pareto points predominate, indicating that hoods may offer a more effective trade-off.

Figure 5b highlights a strong negative linear relationship between C_dA and composite EMG, with Pearson correlation coefficients of $r = -0.96$ for hoods and $r = -0.94$ for drops, indicating robust negative linearity. A linear regression model fitted to the averaged data across participants produced coefficients of determination (R^2) of 0.93 for hoods and 0.91 for drops. These high R^2 values confirm that the regression model effectively captures the linear relationship, indicating that as aerodynamic drag decreases in more aerodynamic postures, muscle activity increases. This trade-off highlights the importance of balancing aerodynamic advantages with physiological demands, as excessive muscle activation in aggressive postures may lead to fatigue. The strong linearity supports the hypothesis of a coupled relationship between drag and muscle activity.

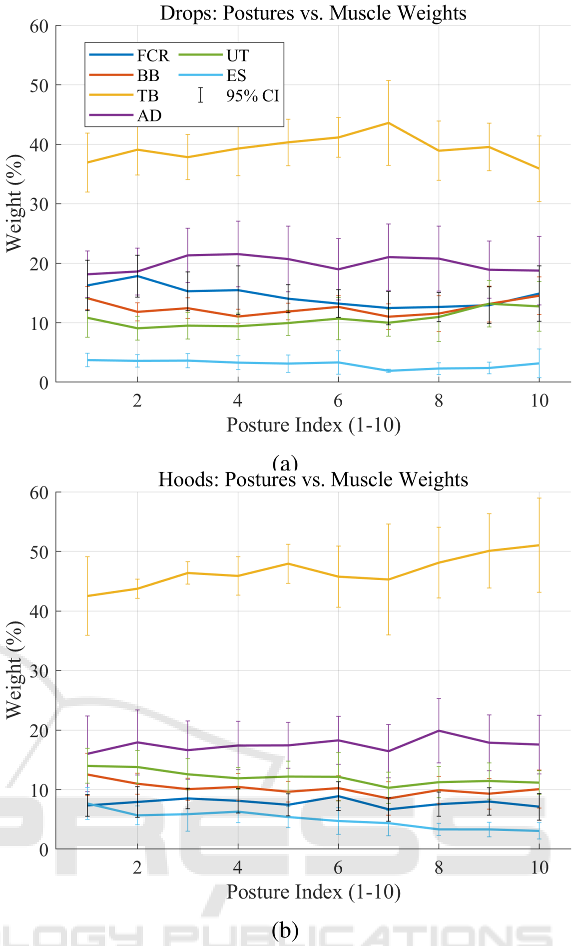

Figure 4: Muscle activation contributions across different postures in (a) hoods and (b) drops position.

4 CONCLUSIONS

This study explored the relationship between aerodynamic drag and upper limb muscle activity to identify optimal cycling postures that balance aerodynamic efficiency with physiological costs. Aerodynamic drag was measured in a controlled wind tunnel across various postures, while upper limb muscle activity was assessed using surface EMG on a bike trainer, repli-

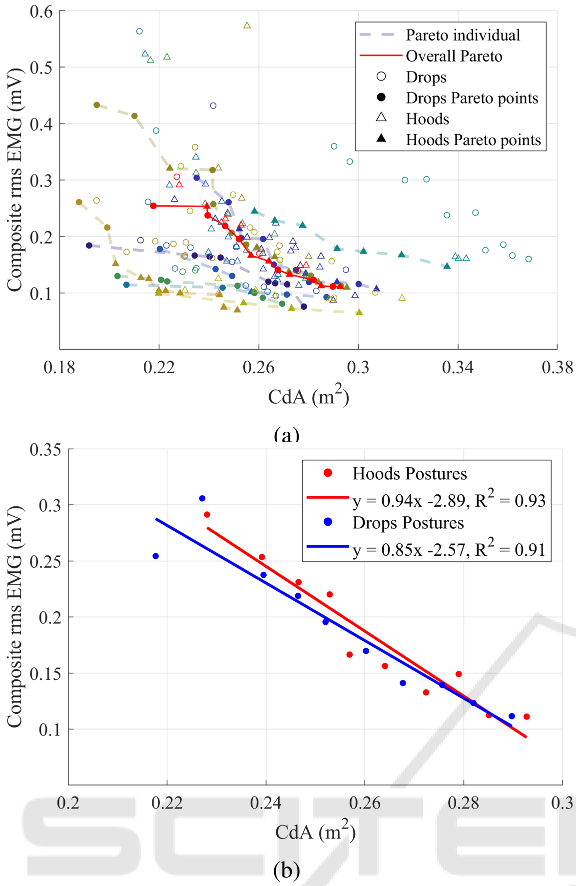

Figure 5: Drag-muscle activity relationship in analysis of (a) Pareto optimality and (b) linear regression for the group. Each color (other than red) in (a) represents data from a participant. Red color denotes group averaged data.

cating the wind tunnel postures. Pareto optimality and linear regression analyses were used to examine the trade-offs between drag and muscle activation.

Drag measurements showed a strong negative correlation between drag area (C_dA) and forearm angle, confirming that more aerodynamic postures significantly reduce drag. However, this benefit comes with increased muscle activation, as demonstrated by EMG data. The triceps brachii was the primary contributor to muscle activation across all postures in both hoods and drops positions. Pareto optimality analysis indicated that drops positions optimize crouched postures, while hoods positions better balance drag and muscle activation in upright postures. This is consistent with linear regression intercepts: in low-drag regions, drops require less muscle activation, but beyond the intersection point, hoods are more efficient for upright postures.

Despite these insights, the study has some limitations. The participant group consisted solely of right-handed male cyclists, and the small sample size and limited number of muscles analyzed restrict the generalizability of the findings. Additionally, individual EMG responses exhibited significant variability, reflecting diverse muscle activation patterns. Pareto optimality analysis further suggested that optimal hand positions vary by individual, supporting the need for personalized bike fitting, as corroborated by Faulkner et al. (Faulkner et al., 2024). Emerging research highlights bidirectional and ipsilateral coupling between upper and lower limb muscle activation in cycling, with greater variability in upper limb activation (Huang and Ferris, 2009; Cartier et al., 2022). Future studies could investigate upper and lower limb coordination to elucidate their combined impact on cycling performance.

The findings offer practical guidance for cyclists and coaches. For time trials prioritizing aerodynamic efficiency, a drops position with a lower forearm angle minimizes drag but increases activation of arm and chest muscles (FCR, BB, AD), necessitating targeted endurance training. For endurance rides prioritizing comfort, a hoods position with a more upright posture reduces activation of shoulder and back muscles (UT, ES), enhancing sustainability. Coaches can use these insights to customize bike fitting and training regimens, balancing aerodynamic benefits with physiological demands. Regular EMG monitoring during training can help identify fatigue thresholds and optimize posture adjustments.

ACKNOWLEDGEMENTS

This work is partially supported by the Hong Kong Innovation and Technology Commission (No.ITS/101/23FP). The author would like to thank HKUST for PhD sponsorship. This work was performed in the Aerodynamics and Acoustics Facility at HKUST (http://aaf.ust.hk).

REFERENCES

Arpinar-Avsar, P., Birlik, G., Sezgin, Ö. C., and Soylu, A. R. (2013). The effects of surface-induced loads on forearm muscle activity during steering a bicycle. *J Sports Sci Med*, 12(3):512.

Ashe, M. C., Scroop, G. C., Frisken, P. I., Amery, C. A., Wilkins, M. A., and Khan, K. M. (2003). Body position affects performance in untrained cyclists. *Br J Sports Med*, 37(5):441–444.

Berry, M. J., Koves, T. R., and Benedetto, J. J. (2000). The influence of speed, grade and mass during simulated off road bicycling. *Appl Ergon*, 31(5):531–536.

Berry, M. J., Pollock, W. E., Van Nieuwenhuizen, K., and Brubaker, P. H. (1994). A comparison between aero and standard racing handlebars during prolonged exercise. *Int J sports Med*, 15(01):16–20.

Bini, R. R., Daly, L., and Kingsley, M. (2019). Muscle force adaptation to changes in upper body position during seated sprint cycling. *J Sports Sci*, 37(19):2270–2278.

Borg, G. A. (1982). Psychophysical bases of perceived exertion. *Med Sci Sports Exerc*, 14(5):377–381.

Brand, A., Sepp, T., Klöpfer-Krämer, I., Müßig, J. A., Kröger, I., Wackerle, H., and Augat, P. (2020). Upper body posture and muscle activation in recreational cyclists: Immediate effects of variable cycling setups. *Res Q Exerc Sport*, 91(2):298–308.

Burden, A. and Bartlett, R. (1999). Normalisation of emg amplitude: an evaluation and comparison of old and new methods. *Med Eng Phys*, 21(4):247–257.

Cartier, T., Vigouroux, L., Viehweger, E., and Rao, G. (2022). Subject specific muscle synergies and mechanical output during cycling with arms or legs. *PeerJ*, 10:e13155.

Chapman, A. R., Vicenzino, B., Blanch, P., Knox, J. J., Dowlan, S., and Hodges, P. W. (2008). The influence of body position on leg kinematics and muscle recruitment during cycling. *J Sci Med Sport*, 11(6):519–526.

Dettori, N. J. and Norvell, D. C. (2006). Non-traumatic bicycle injuries: a review of the literature. *Sports Med*, 36(1):7–18.

Dorel, S., Couturier, A., and Hug, F. (2009). Influence of different racing positions on mechanical and electromyographic patterns during pedalling. *Scand J Med Sci Sports*, 19(1):44–54.

Ehrgott, M. (2005). *Multicriteria optimization*, volume 491. Springer Science & Business Media.

Faria, E. W., Parker, D. L., and Faria, I. E. (2005). The science of cycling: factors affecting performance—part 2. *Sports Med*, 35:313–337.

Faulkner, S. H. and Jobling, P. (2020). The effect of upper-body positioning on the aerodynamic–physiological economy of time-trial cycling. *Int J Sports Physiol Perform*, 16(1):51–58.

Faulkner, S. H., Jobling, P., Griggs, K. E., and Siegkas, P. (2024). Individual aerodynamic and physiological data are critical to optimise cycling time trial performance: one size does not fit all. *Sports Eng*, 27(1):4.

Fintelman, D., Sterling, M., Hemida, H., and Li, F. (2014). Optimal cycling time trial position models: aerodynamics versus power output and metabolic energy. *J Biomech*, 47(8):1894–1898.

Fintelman, D., Sterling, M., Hemida, H., and Li, F. (2015). The effect of time trial cycling position on physiological and aerodynamic variables. *J Sports Sci*, 33(16):1730–1737.

Ghasemi, M., Curnier, D., Caru, M., Trépanier, J.-Y., and Périé, D. (2022). The effect of different aero handlebar positions on aerodynamic and gas exchange variables. *J Biomech*, 139:111128.

Giljarhus, K. E. T., Stave, D. Å., and Oggiano, L. (2020). Investigation of influence of adjustments in cyclist arm position on aerodynamic drag using computational fluid dynamics. *Proc*, 49(1):159.

Huang, H. J. and Ferris, D. P. (2009). Upper and lower limb muscle activation is bidirectionally and ipsilaterally coupled. *Med Sci Sports Exerc*, 41(9):1778.

Ingraham, K. A., Ferris, D. P., and Remy, C. D. (2019). Evaluating physiological signal salience for estimating metabolic energy cost from wearable sensors. *J Applied Physiology*, 126(3):717–729.

Kordi, M., Fullerton, C., Passfield, L., and Parker Simpson, L. (2019). Influence of upright versus time trial cycling position on determination of critical power and w in trained cyclists. *Eur J Sport Sci*, 19(2):192–198.

Mao, J., Zhou, P., Liu, G., Zhong, S., Huang, X., and Zhang, X. (2024). The influence of crosswinds and leg positions on cycling aerodynamics. *Exp Fluids*, 65(6):85.

Martin, J. C., Gardner, A. S., Barras, M., and Martin, D. T. (2006). Modeling sprint cycling using field-derived parameters and forward integration. *Med Sci Sports Exerc*, 38(3):592–597.

Pareto, V. (1919). *Manuale di economia politica con una introduzione alla scienza sociale*, volume 13. Società Editrice Libraria.

Savelberg, H. H. C. M., Van de Port, I. G. L., and Willems, P. J. B. (2003). Body configuration in cycling affects muscle recruitment and movement pattern. *J Appl Biomech*, 19(4):310–324.

Schwellnus, M. P. and Derman, E. W. (2005). Common injuries in cycling: Prevention, diagnosis and management. *S Afr Fam Pract*, 47(7):14–19.

So, R. C., Ng, J. K. F., and Ng, G. Y. F. (2005). Muscle recruitment pattern in cycling: a review. *Phys Ther Sport*, 6(2):89–96.

Stegeman, D. and Hermens, H. (2007). Standards for surface electromyography: The european project surface emg for non-invasive assessment of muscles (seniam). *Enschede: Roessingh Research and Development*, 10(8).

Turpin, N. A., Costes, A., Moretto, P., and Watier, B. (2017). Upper limb and trunk muscle activity patterns during seated and standing cycling. *J Sports Sci*, 35(6):557–564.

Umberger, B. R., Scheuchenzuber, H. J., and Manos, T. M. (1998). Differences in power output during cycling at different seat tube angles. *J Hum Mov Stud*, 35(1):21–36.